



Instrument Science Report NICMOS 2008-01

Bright Earth Persistence in NICMOS

A. Riess, E. Bergeron
March 20, 2008

ABSTRACT

We report the presence of image persistence in NICMOS data due to prior saturation of the array by the bright Earth as well as an algorithm to remove its impact. BEP (Bright Earth Persistence) may occur when ACS and NICMOS are used in parallel, and the data dump of ACS delays the insertion of the NICMOS filter blank as long as 6 minutes beyond the Bright Earth avoidance angle. We have constructed a BEP frame which can be used to model and remove the presence of BEP in NICMOS data. The algorithm is seen to remove 99.5% of the variance in the background of BEP impacted Camera 2 data. Ongoing work involves broadening the applicability of the BEP correction to Camera 1 and 3 and making it available as a pyraf script through STSDAS.

Introduction

The NICMOS detectors have exhibited a long list of anomalies over their 10 years on HST including: Amplifier Glow, Bias Jumps (in bands), Cosmic Ray Persistence, Count-rate Non-linearity, Electronic Ghosts, Optical Ghosts, Particulate Contaminants, Residual Bias, Shading, and Vignetting, to name just a subset (see <http://www.stsci.edu/hst/nicmos/performance/anomalies>) for a full list. Here we present still another NICMOS anomaly, Bright Earth Persistence, which results from the combination of a well known NICMOS problem (image persistence with multiple trap decay timescales) coupled to a different source of excitation (the bright Earth instead of cosmic rays or astronomical sources as previously documented in

(CALIBRATION WORKSHOP 97 -- Persistence in NICMOS: Results from On-Orbit data. and NICMOS ISR 98-001 Najita, Dickinson, Holfeltz 1998).

The significance of the impact of bright Earth persistence (hereafter BEP) came to our attention from the SHOES program (GO 10802, PI: A. Riess, Cycle 15). The SHOES program utilizes NIC2 with F160W to observe clusters of Cepheids in hosts of nearby type Ia supernovae. In the course of data collection, visit B2 presented an unusual large-scale pattern of elevated sky level. It was not recognized as one of the “classic” NICMOS anomalies, nor frequently seen by even the most experienced NICMOS analyst¹. Large-scale patterns in the sky background which resemble the dark or flat-field can result from the temperature-dependence of the dark current (and the subtraction of a dark frame of improper temperature) or by the use of a flat-field lamp in lieu of a sky flat (the color of whose flux will affect the quantum efficiency of the detectors) but this pattern resembled neither the flat nor the dark. We concluded that the pattern resulted from image persistence by observing its exponential decay (about 20% every 400 seconds) during the course of the orbit.

An investigation of the SMS showed visit B1 from the same program was acquired just prior to B2 and had no evidence of the pattern. There was no slewing of the telescope between these visits. At the end of the B1 integration, the ACS dump to the solid state recorder preceded the NICMOS dump, delaying the NICMOS transition from “observe” to “operate” and the accompanying placement of the filter blank (NICMOS has no shutter) for 6 minutes beyond occultation by the bright Earth. Ordinarily, NICMOS waits for 10 minutes after the most recent NICMOS activity before inserting the filter blank. Thus NICMOS was seeing the Bright Earth through F160W for 45 seconds to 70 seconds prior to visit B2. The Earth’s flux saturated the array, filling the traps to capacity. The B1 exposures are unaffected because these data reside in the buffer, waiting to be transmitted to the SSR. At the start of B2, each read-out contains charge decaying from the trapped state and back into the bulk of the pixels. The resulting “persistence image” is thus a decaying map of the trap density in the detector.

The “good news” is that the effect of BEP is easy to determine and remove with little residual impact to quantitative information in the image.

Here we explain how we characterized the NICMOS BEP and corrected impacted NICMOS images.

Bright Earth Persistence

Further investigation of the SHOES program data yielded 10 clear examples of BEP which we could use to characterize the 2-dimensional persistence image. For each of these examples we were able to identify a matching frame of the same field from the SHOES program without any detectable BEP. We registered the unaffected images to

¹ E. Bergeron, 02/14/2007, “I’m excited to say, I’ve never seen an image like that in my life.”

the BEP-impacted frames and subtracted the former to remove the sources and the mean sky. A combination of these produced an average persistence frame. The visit pairs we used are given in Table 1.

Table 1: Visit Pairs from GO 10802 used to Derive the BEP Image

Target Field	BEP Visit	Matching visit w/o BEP
NGC3370_green	B2	B1
NGC3021_cyan	6F	6E
NGC1309_cyan2	5D	5J
NGC1309_green	59	5A
NGC4639_cyan	1E	1D
NGC4536_blue	24	25
NGC3982_blue	35	3G
NGC3021_red	62	6H
NGC3021_green	6B	6A
NGC4536_green	27	28

The averaged persistence frame is shown in Figure 1. Its normalization is arbitrary and unimportant as it will be used to scale as needed and subtract from frames. However, for the following it may be useful to consider that a unity scaling of this frame represents the level of BEP seen by the middle of the orbit immediately following a hard, bright Earth flash at the beginning of the preceding occultation. At the start of the orbit, the level of BEP can exceed twice this level and by the end approximately half this level. The average level of this BEP frame is 0.047 e/s, similar to the average sky level.

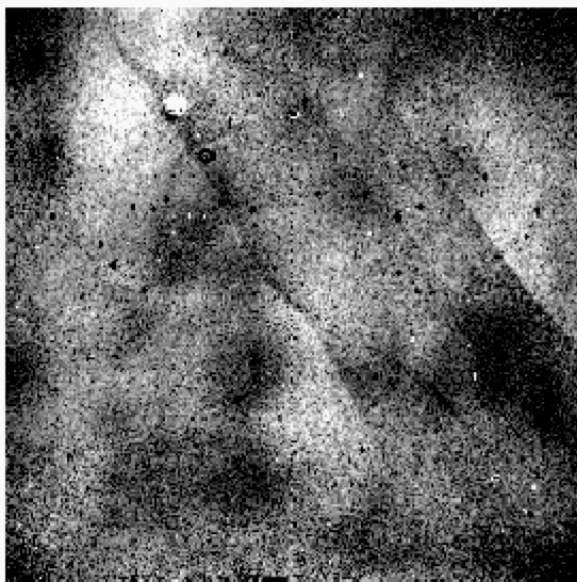


Figure 1: BEP image derived from combining the 10 BEP impacted visits in Table 1 from the SHOES program (GO 10802) after removal of sources using a matching non-BEP impacted visit. Small scale features like such as “grot” remain because the offsets between visits move these features relative to the registered sky sources.

One can see small-scale features (e.g., grot) remain in the BEP image due to dithering or guide star reacquisition variations between pairs of images used to remove sources.

Figure 2 compares the BEP frame of Camera 2 to the trap map derived from cosmic ray persistence (i.e., from a combination of all post-SAA darks) and a lamp persistence image derived from long dark frames (at least 30 seconds for sufficient signal) immediately following the use of the bright lamp for flats (from GO 10728). The large-scale features in all of these are similar, demonstrating that the *source* of excitation leading to trap filling is not important. Rather, it’s the two-dimensional structure and variation in trap density which determines the characteristics of the persistence image. This structure is

common to all impacted images. We note that the BEP image from SHOES has a superior signal-to-noise ratio because the saturation of the detector is more complete (the Earth is brighter than the lamp and provides better coverage than CR's) and the subsequent exposures were 1000's of seconds. We speculate that the additional charge seen at the edges (Figure 2: middle panel) results from the larger unshielded solid angle these pixels see for cosmic rays than for photons.

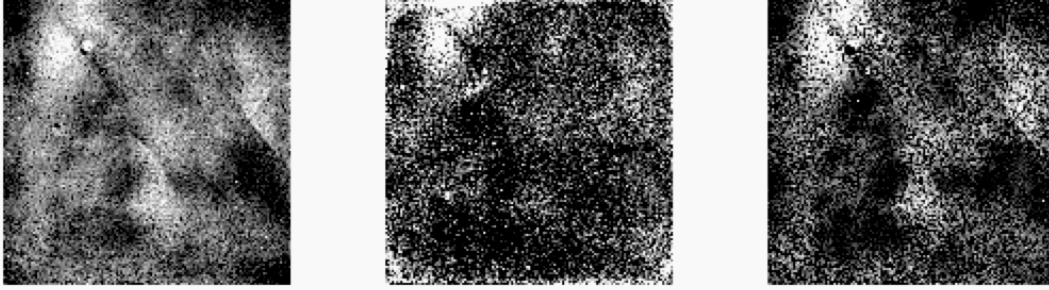


Figure 2: NIC2 Persistence images: The far left is the BEP image derived from the 10 impacted visits of the SHOES program. The middle panel is the persistence seen from the peppering of the full detector by CR hits in numerous SAA passages. The version on the right, like SHOES, is caused by persistence from photons, in this case after the use of the lamps. The best signal-to-noise ratio for modeling the persistence comes from the BEP on the left due to its more uniform and greater excitation.

Removal of BEP

The presence of BEP in an image is a nuisance, adding a mottled and irregular sky pattern which, uncorrected, can lead to difficulty in determining the sky level underneath a source and resulting in errors in photometry. BEP may also change source shapes and structure, and elevate sky noise from the Poisson statistics of trap decays. However, it has been shown elsewhere (Bergeron and Dickinson 2003, ISR 2003-10) that persistence can effectively be removed from the impacted frame with the use of a persistence image. The formalism used for removal of CR persistence in post-SAA images (coded in the algorithm *SAAClean*) is to seek and subtract the fraction of a post-SAA dark frame which minimizes the variance of the sky. This works well for the sporadic and small-scale features of cosmic ray impacts because the sky noise is only elevated around the CR impact. For regions of the image devoid of CR impacts, there is no additional sky noise to reduce. In contrast, *the entire image* in a BEP-impacted frame contains information about the level of BEP. Therefore, instead of minimizing residuals relative to adjacent pixels, we seek to minimize residuals relative to a flat sky, sans sources.

We set up the problem as follows:

$$y_i = s + Px_i + n_i$$

where y_i is the set of pixels (at pixel location i) of the original frame without source pixels included, s is the sky level, P is the persistence level, x_i is the same set of pixels of the BEP frame, and n_i are the residuals of the model. We set up this relation as a system of equations using the following matrix:

$$\begin{bmatrix} y_1 \\ y_2 \\ \vdots \\ y_N \end{bmatrix} = \begin{bmatrix} 1 & x_1 \\ 1 & x_2 \\ \vdots & \vdots \\ 1 & x_N \end{bmatrix} \cdot \begin{bmatrix} s \\ P \end{bmatrix} + \begin{bmatrix} n_1 \\ n_2 \\ \vdots \\ n_N \end{bmatrix}$$

The least-squares estimator, i.e., the parameters which minimize the sum of the square of data minus model, is given immediately by matrix inversion:

$$\delta = (X^T X)^{-1} X^T Y$$

so that the best estimate of δ =[sky,persistence].

Before performing the BEP correction we run *calnica* and the *pedsub* procedure to produce a calibrated frame free of quad amp offsets. Then we identify the pixels we will mask for exclusion from the BEP model.

We combined the standard NICMOS bad pixel list with the 35x35 pixels in the corners (to avoid amp glow) and add to that the individual source pixels identified. The small-scale source pixels we mask are those which exceed four standard deviations in the difference between the image and a *ringmedian* (inner=3 outer=6) version of the image. To avoid larger source features (e.g., nebulae or diffuse emission) in the modeling we also masked pixels which exceeded 150% of the median level of the original image. For an image with typical sky and unity level of BEP, this limit corresponds to a positive 3 standard deviation cut above the noise. Our BEP frame is also a ringmedian version of

the one shown in Figure 1 (to avoid the grot and small scale features which are not part of BEP). An important advantage of using a smoothed version of the BEP is that it reduces the noise in the frame while retaining the basic BEP features.

As a test case we ran all of the SHOES data, consisting of approximately 50 different crowded scenes of nearby galaxies. On average, the masking retained about 85% of the pixels for BEP modeling. The results for 21 SHOES visits are shown in Figure 3. The upper panel shows the BEP scale, the middle panel the sky level, and the lower panel shows the fraction of pixels used in the fit. Two examples typical of the result of subtracting a significant fraction of the BEP model are shown in Figure 4. As shown, this procedure provides a substantial improvement in obtaining a uniform background.

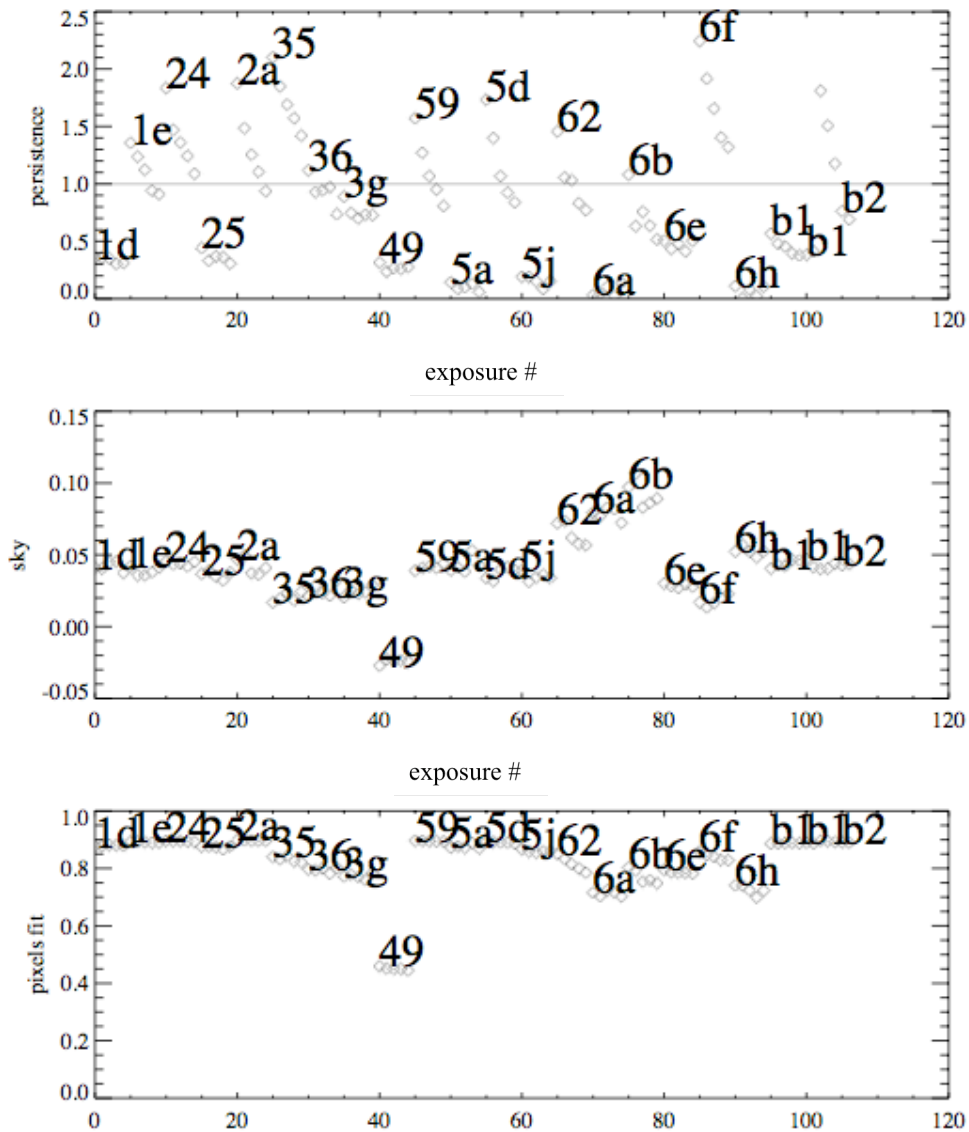


Figure 3: Results of modeling 21 visits of the SHOES program. The upper panel shows the persistence level. Visits for which the persistence is above ~ 0.5 and especially those for which the level decays in time have been strongly impacted by BEP.

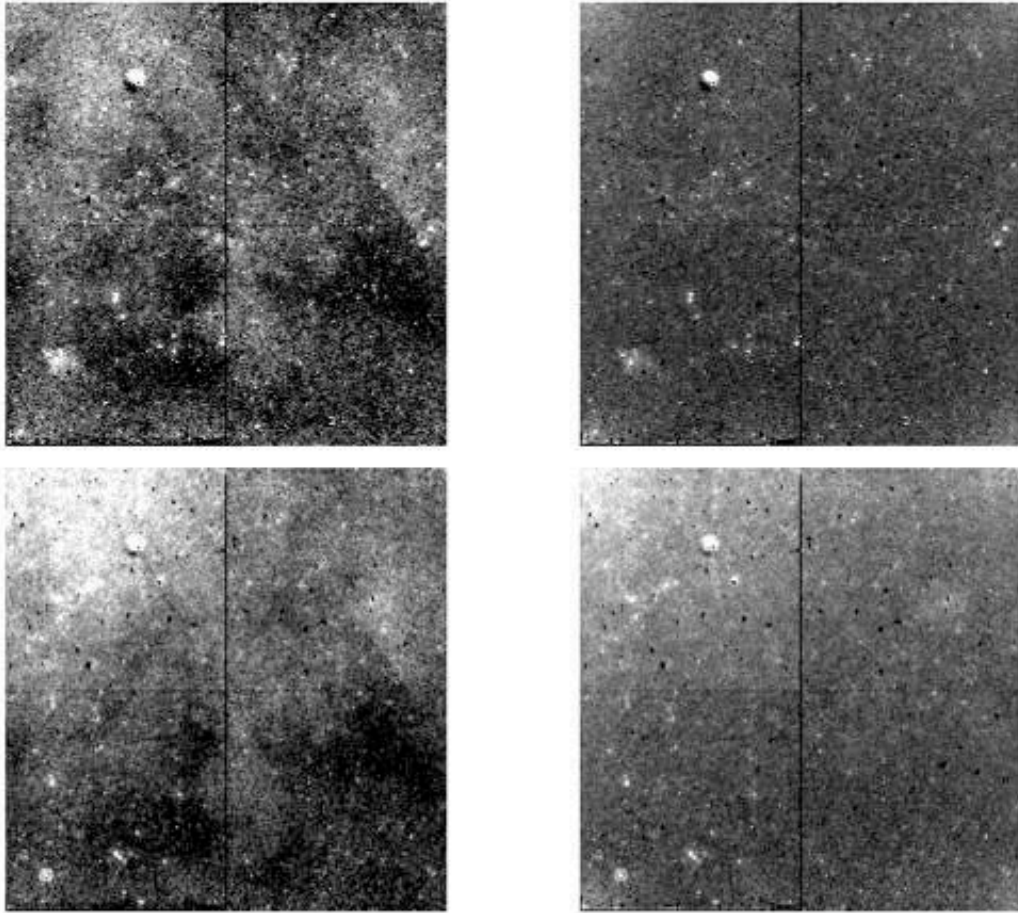


Figure 4: Two typical examples of BEP correction. Left upper panel is the first dither of visit B2 and lower panel is first dither of visit 35 from GO 10802. To the right are the same after the removal of BEP.

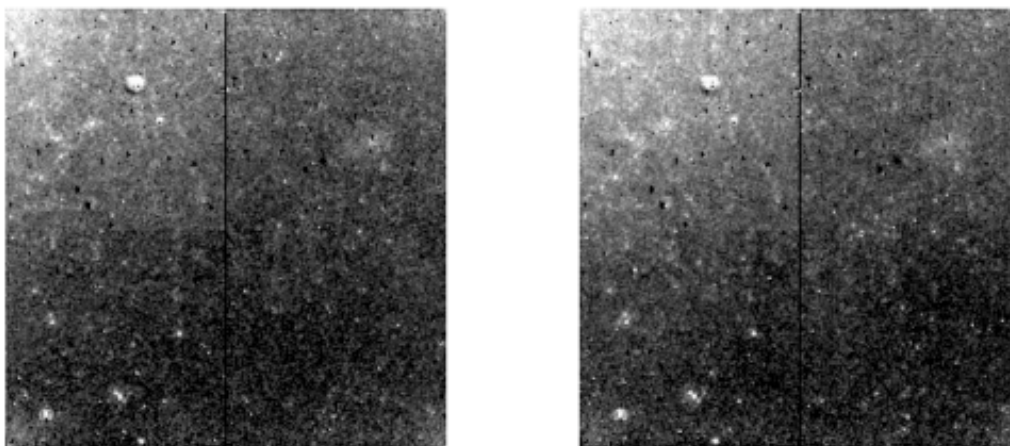


Figure 5: A BEP-corrected image versus the same field in the absence of any BEP. Left, first dither of visit 35 after a high level of BEP removal. Right, first dither of visit 36 in which negligible BEP was present.

The most efficient method for finding other programs impacted by BEP is to perform the BEP modeling and consider the value of the persistence parameter. Remaining, unmasked features in a field presently cause this parameter to vary with a full range of ± 0.5 in the absence of BEP. Especially difficult to model are very crowded fields where it is difficult to identify more than 50% of the pixels unique to the background. We find that for persistence values less than 0.5 (of the persistence frame) or background pixel fractions of less than 50%, BEP should not be removed because of the risk of doing more harm than good. Images near these conditions should be visually inspected to determine the best course of action. Persistence values greater than 0.5 and especially those accompanied by a decay of the persistence level across the orbit are almost certain to arise from BEP and may be dramatically improved by the removal of the modeled BEP.

A Case Study, GO 10258

As an independent test case, we considered the program GO 10258 (P.I. C. Kretchmer), a series of NIC2 pointings in the GOODS fields with ACS observing in parallel. Parallel use of ACS and NICMOS followed by an orbit using NICMOS is a good candidate for BEP due to the long data dumps of ACS which can cause NICMOS to remain in observe

mode, staring at the bright Earth. A program with multi-orbit visits of ACS and NICMOS in parallel is a good candidate to look for this set of circumstances. In addition, it is especially easy to recognize BEP in sparse extragalactic fields such as GOODS, even more so than in the crowded fields of the SHOES program.

The results of our search for BEP in the 20 visits of GO 10258 are shown in Figure 6.

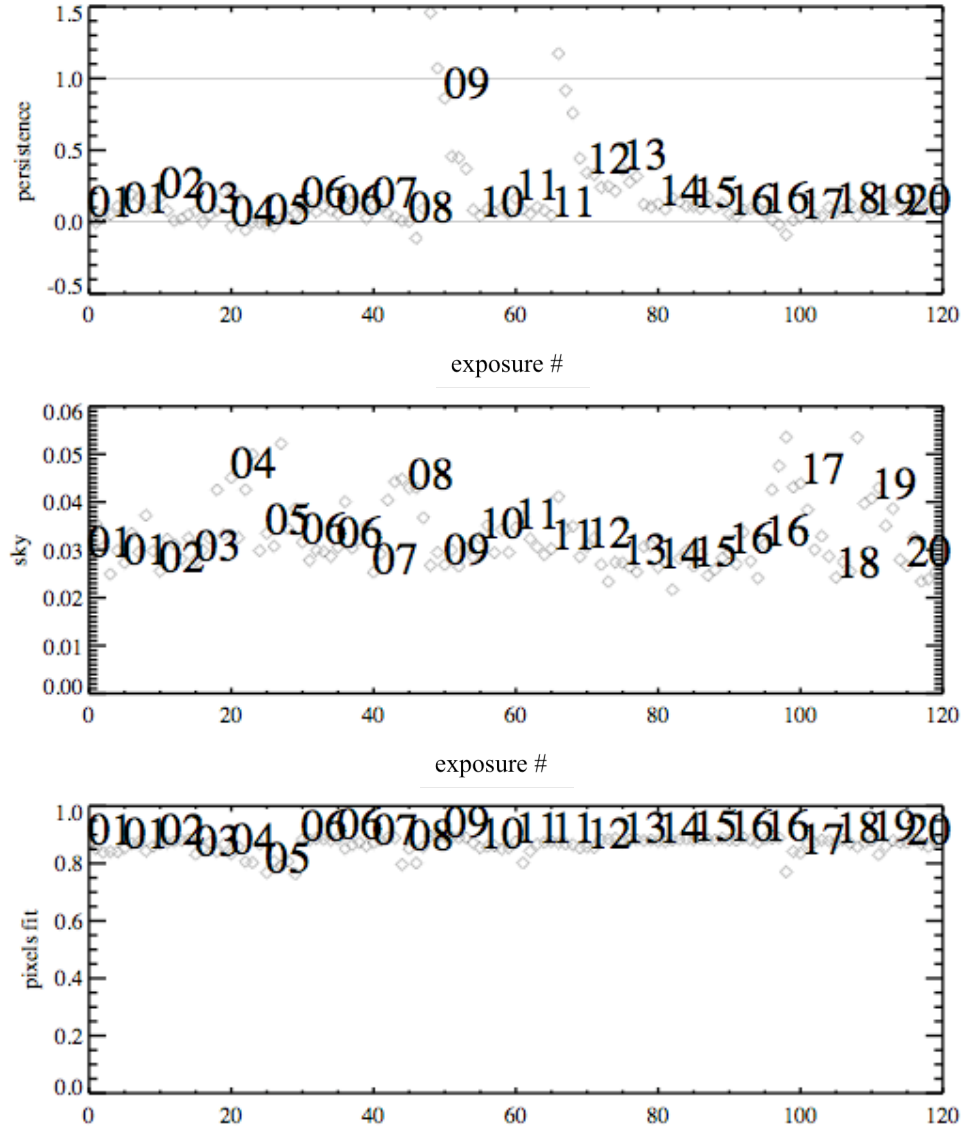


Figure 6: Search for BEP impacted images from GO 10258 (P.I. Kretchmer), NIC2 imaging in the GOODS fields. These extragalactic fields provide for very straightforward BEP modeling with $\sim 90\%$ of pixels useful for the fit (lowest panel). Two visits, 9 and 12, show a clear signature of BEP, both by level and time decay.

These relatively sparse fields are easy to model with typically 90% of the pixels useable. In 18 of the 20 visits shown the persistence level is extremely low, about 0.1 or less, a

value which we conclude is negligible. The exceptions are visits 9 and 12 for which the first dither has a persistence level greater than one with a clear decay between every dither ending at a level of ~ 0.3 for the last, one-fifth of the first. In Figure 7 we show the first dither of these two visits, before and after the BEP correction. The improvement is substantial and has removed 99.5% of the image variance in visit 9 (upper row). However, we note that the BEP removal is not perfect. There appears to be a very slight depression in the flux level in the lower left quadrants. Although this feature is present in the BEP image, additional subtraction might have caused a depression in the upper left quadrant due to the bright feature in the BEP frame. The modeling is trying to find the best compromise. At this level there are a number of reasons for imperfection which may be addressed in the future including: a variation in BEP due to the angle of Earth illumination, a temperature sensitivity to trapping or the subtleties of removing a source of charge insensitive to pixel quantum efficiency together with the sky and scene (Eddie?)

Without analyzing a fair fraction of past NICMOS data, we cannot yet know the frequency with which BEP occurs during NICMOS imaging. However, it's clear that the frequency will be a strong function of observing parameters including instruments used in parallel and the length of the observation. For the SHOES program and the 10258 program it was 5% and 10%, respectively (both of which used ACS in parallel).

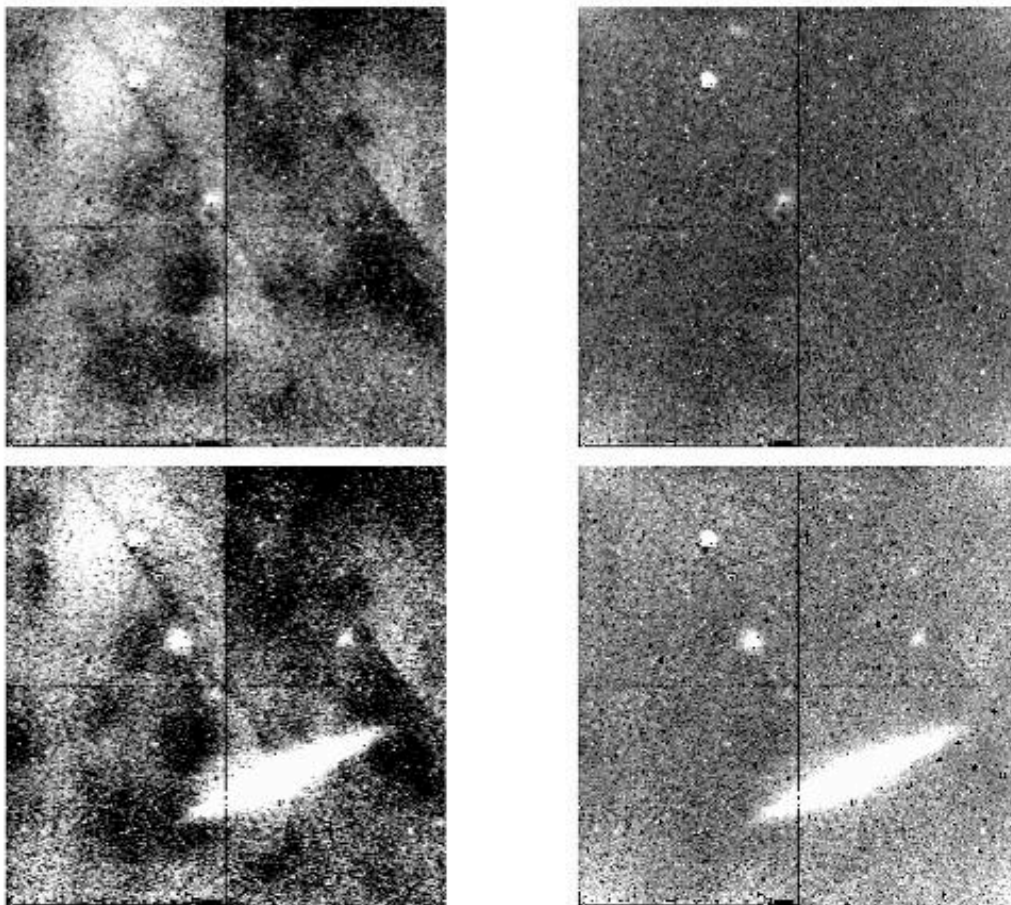


Figure 7: Two BEP impacted dithers from GO 10258, visit 9 (upper) and visit 12 (lower). The corrected images (right) have the variance of their background reduced by 99.5%. Residuals are discussed in the text.

Camera 1 and 3

We have focused on the effect of BEP on Camera 2 because this is the camera in which it was first noticed and our experience was gained by removing it from the SHOES data. However, it's very likely that both Camera 1 and 3 suffer BEP as well. To provide guidance in identifying and correcting BEP in those cameras we determined the BEP structure from CR impacts in post-SAA darks and from post-lamp darks. These are shown in Figure 8 (Camera 1: upper row and Camera 3: lower row).

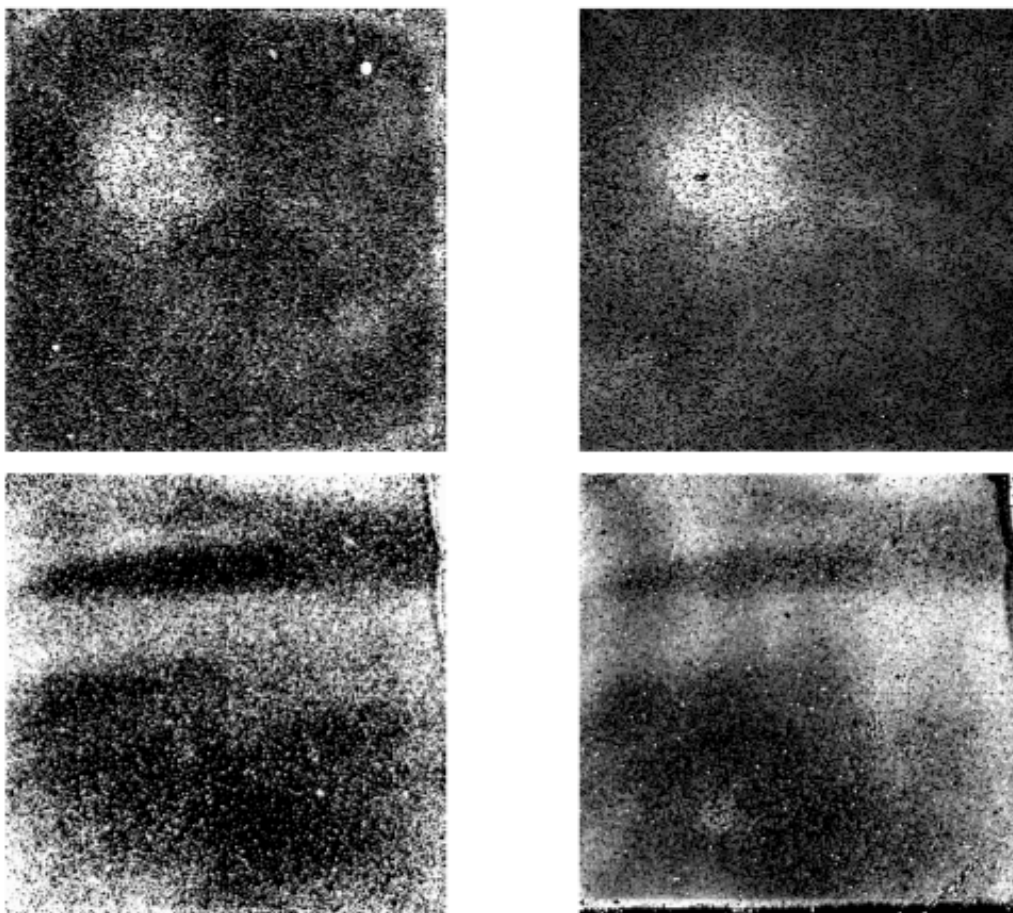


Figure 8: The expected structure of BEP in Camera 1 and 3. On the left is the Camera 1 (top) and Camera 3 (bottom) persistence image inferred from post-SAA darks (i.e., cosmic rays). On the right is the same from the post-lamp darks.

Recommendations

Because of the time dependence of the decay of BEP, it may be valuable to fit for the temporal function and perform a simultaneous fit to all of the dithers of an orbit, using a single persistence level parameter. It would be important to verify that the fit works equally well across the dither. Such an approach would be especially valuable for removing the BEP at the end of an orbit when the level is small enough to become relatively uncertain. A simple way to do this would be to add the additional dithers to the matrix equation, and expand the persistence term, P , to $P_0 * P(t)$. One could derive the temporal function, $P(t)$, independently from the post-SAA CR decay function (Bergeron and Dickinson 200X) or from some of the BEP impacted visits. Using the time, t , in the middle of the orbit, and replacing x_i with $x_i P(t)$ in the matrix would allow one to solve for P_0 for the whole orbit.

Acknowledgements

We thank Megan Sosey, Dave Grumm, Helene McLaughlin, and Deepashri Thatte for their efforts to verify the BEP algorithm described here.

References

Bergeron and Dickinson 2003, ISR 2003-10